Environmental Science & Technology LETTERS

Letter

Cite This: Environ. Sci. Technol. Lett. XXXX, XXX, XXX−XXX

pubs.acs.org/journal/estlcu

Brown Carbon Formation from Nighttime Chemistry of Unsaturated Heterocyclic Volatile Organic Compounds

Huanhuan Jiang,[†,∥] Alexander L. Frie,[†,∥] Avi Lavi,[‡] Jin Y. Chen,[§] Haofei Zhang,[‡,§] Roya Bahreini,[†,‡,§] and Ying-Hsuan Lin*[,†,§]

[†]Department of Environmental Sciences, University of California, Riverside, California 92521, United States

[‡]Department of Chemistry, University of California, Riverside, California 92521, United States

[§]Environmental Toxicology Graduate Program, University of California, Riverside, California 92521, United States

Supporting Information

ABSTRACT: Nighttime atmospheric processing enhances the formation of brown carbon aerosol (BrC) in biomass burning plumes. Heterocyclic compounds, a group of volatile organic compounds (VOCs) abundant in biomass burning smoke, are possible BrC sources. Here, we investigated the nitrate radical (NO_3)-initiated oxidation of three unsaturated heterocyclic compounds (pyrrole, furan, and thiophene) as a source of BrC. The imaginary component of the refractive index at 375 nm (k_{375}), the single scattering albedo at 375 nm (SSA_{375}), and average mass absorption coefficients ($\langle MAC \rangle_{290-700\ nm}$) of the resulting secondary organic aerosol (SOA) are reported. Compared to furan and thiophene, NO_3 oxidation of pyrrole has the highest SOA yield. Pyrrole SOA (k_{375} = 0.015 ± 0.003, SSA = 0.86 ± 0.01, $\langle MAC \rangle_{290-700\ nm}$ = 3400 ± 700 $cm^2\ g^{-1}$) is also more absorbing than furan SOA ($\langle MAC \rangle_{290-700\ nm}$ = 1100 ± 200 $cm^2\ g^{-1}$) and thiophene SOA (k_{375} = 0.003 ± 0.002, SSA_{375} = 0.98 ± 0.01, $\langle MAC \rangle_{290-700\ nm}$ = 3000 ± 500 $cm^2\ g^{-1}$). Compared to other SOA systems, MACs reported in this study are higher than those from biogenic precursors and similar to high-NO_x anthropogenic SOA. Characterization of SOA molecular composition using high-resolution mass spectrometric measurements revealed unsaturated heterocyclic nitro products or organonitrates as possible chromophores in BrC from all three precursors. These findings reveal nighttime oxidation of fire-sourced heterocyclic compounds, particularly pyrrole, as a plausible source of BrC.

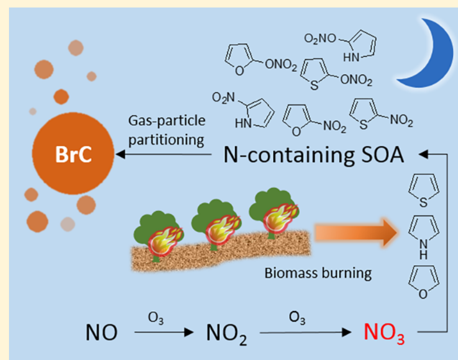

1. INTRODUCTION

Aerosol's radiative effects are the most uncertain components of current climate models.[1] One of the drivers of this uncertainty is the incomplete understanding of aerosol formation and aging processes that influence aerosol's chemical composition and optical properties. Light-absorbing organic aerosols, known as brown carbon (BrC), are estimated to account for ∼20% of aerosol-driven atmospheric heating.[2] The chemical nature of BrC chromophores has been the focus of many recent studies, with field, laboratory, and modeling studies identifying aromatics, conjugated systems, and highly functionalized species, such as organic nitrates, as moieties responsible for absorption of tropospheric solar radiation.[2−16] Specifically, nitroaromatic compounds have been recognized as significant components of BrC.[13]

One previously unexplored pathway of BrC and nitroaromatic formation is the nitrate radical (NO_3)-initiated oxidation of unsaturated heterocyclic compounds. Unsaturated heterocyclic compounds contain heteroatoms (N, O, and S) within their ring structures and represent a unique family of reactive compounds. These compounds are emitted during biomass burning events, with estimated emission factors of 5−37% of total emitted carbon for furans.[17] High levels of NO_x emissions in biomass burning plumes can readily react with O_3 to form NO_3 radicals, the dominant atmospheric oxidant during nighttime.[14,18,19] Thus, heterocyclic compounds and NO_3 radicals are likely to co-occur in the nighttime atmosphere. Major unsaturated heterocyclic compounds are known to react quickly with NO_3 radicals,[20] forming condensable nitro- or nitrate-containing reaction products that are likely to absorb light in the UV−visible range.[7,10,21]

Here, the NO_3 oxidation of unsaturated heterocyclic compounds is investigated as a probable and previously unrecognized source of BrC. Through a series of chamber experiments, we characterized chemical and optical properties of SOA from NO_3-initiated oxidation of pyrrole, furan, and thiophene as model compounds for five-membered unsaturated heterocyclic compounds. We used both online and offline techniques to evaluate single scattering albedo (SSA, λ

Received: January 8, 2019
Revised: January 28, 2019
Accepted: January 30, 2019
Published: January 30, 2019

DOI: 10.1021/acs.estlett.9b00017
Environ. Sci. Technol. Lett. XXXX, XXX, XXX−XXX

Table 1. Summary of Experimental Conditions

precursor	$[O_3]_{eq}$ [a]	$[NO_x]_{eq}$ [b] (ppb)	AM_{max} [c] (μg m^{-3})	average $AAE_{290/400}$ [d]	average $AAE_{400/600}$ [d]	average ⟨MAC⟩ (cm^2 g^{-1}) [e]	n_{375} [f]	k_{375} [f]	SSA_{375} [g]
pyrrole	750	350	558	5.59 ± 1.43	7.86 ± 0.45	3400 ± 700	1.41 ± 0.03	0.017 ± 0.002	0.86 ± 0.01
pyrrole	1200	300	770				1.34 ± 0.04	0.013 ± 0.002	0.86 ± 0.01
pyrrole	1160	310	615				1.40 ± 0.01	0.014 ± 0.003	0.87 ± 0.01
furan	590	330	17	6.43 ± 0.76	5.42 ± 0.36	1100 ± 200	h	h	h
furan	560	160	43						
furan	800	170	47						
thiophene	530	350	264	5.70 ± 0.35	7.60 ± 0.75	3000 ± 500	1.44 ± 0.01	0.003 ± 0.002	0.98 ± 0.01
thiophene	420	280	218				1.45 ± 0.01	0.002 ± 0.001	0.98 ± 0.01
thiophene	750	330	285				1.47 ± 0.02	0.003 ± 0.002	0.98 ± 0.01

[a] $[O_3]_{eq}$: the measured equilibrium O_3 concentration. [b] $[NO_x]_{eq}$: the measured equilibrium NO_x concentration. [c] AM_{max}: the maximum aerosol mass concentration during the experiment. [d] Average $AAE_{290/400}$, $AAE_{400/600}$: the average absorption Ångström exponent in the UV range and visible range, respectively, expressed as mean of triplicate experiments ± the corresponding standard deviation. [e] Average ⟨MAC⟩: the average ⟨MAC⟩ value calculated from triplicate experiments ± the corresponding standard deviation. [f] n_{375} and k_{375}: the averaged n_{375} and k_{375} over the experiment when mode changed <10% in consecutive SEMS runs and optical coefficients were above PAX detection limits. [g] SSA_{375}: the averaged SSA_{375} over the experiments when $x_{375} > 1$. [h] During the furan experiment, more than 50% of $\beta_{abs,375}$ measurements were below the PAX detection limit with the remaining values being only marginally higher. Thus, n_{375}, k_{375}, and SSA_{375} were not reported for furan experiments.

= 375 nm), refractive index (RI, λ = 375 nm), and mass absorption coefficients (MAC, 290−700 nm) to provide a broad picture of the optical characteristics of SOA. Molecular composition of SOA was analyzed to identify potential chromophores.

2. MATERIALS AND METHODS

2.1. Controlled Chamber Experiments. Experiments were performed under dry conditions (RH = 2−16%) within a ~1.3 m^3 FEP Teflon chamber located at the University of California, Riverside. Before each experiment, the chamber was filled with zero air (Airgas). O_3 was generated through corona discharge (Enaly, 1000BT-12) and injected into the chamber until a concentration of ~1500 ppbv O_3 was reached. Next, 2 L of NO (Praxair, 482 ppmv in air) was injected into the chamber. The chamber was equilibrated for an hour to allow reservoirs of NO_3 and N_2O_5 to develop. As shown in Supporting Information (SI), Figure S1, more than 9 ppbv NO_3 can be generated after 1 h as simulated using a kinetic box model.[22−24] Then, pyrrole (TCI America, >99%), furan (TCI America, >99%), or thiophene (Alfa Aesar, 99%) was added into a glass bulb and the vapors were introduced into the chamber by flowing ultrazero air (Aadco Instruments Inc., 747-30) through the bulb to achieve an effective chamber concentration of ~200 ppbv. Under these conditions, the oxidation of all precursors is dominated by the NO_3 pathway as shown in the SI, section S1 and Table S1. Aerosol size distributions, NO_x (NO + NO_2) and O_3 were continuously monitored during experiments with a scanning electron mobility spectrometer (SEMS, Brechtel Manufacturing Inc.), NO_x analyzer (Thermo 42i-LS), and an O_3 analyzer (Thermo 49i), respectively. A summary of experimental conditions is provided in Table 1.

2.2. Online Chemical and Optical Characterization. Gas-phase reaction products were analyzed in real time by an iodide-adduct high-resolution time-of-flight chemical ionization mass spectrometer (HR-ToF-CIMS, Tofwerk AG, Aerodyne Research Inc.). Additional details are described in SI, section S2.

Scattering and absorption coefficients at 375 nm ($\beta_{scat,375}$ and $\beta_{abs,375}$) were measured at 1 Hz using a photoacoustic extinctiometer (PAX) (Droplet Measurement Technologies, Boulder, CO). PAX measurements were averaged to the SEMS scan time (140 s). PAX detection limits, defined as 3 times the standard deviation of scattering and absorption measurements of filtered air averaged to 140 s, were 1.29 and 1.08 Mm^{-1}, respectively, for $\beta_{scat,375}$ and $\beta_{abs,375}$. The single scattering albedo at 375 nm (SSA_{375}) was calculated using eq 1.

$$SSA_{375} = \frac{\beta_{scat,375}}{\beta_{scat,375} + \beta_{abs,375}} \qquad (1)$$

The size parameter (x) is useful in understanding SSA dynamics due to SSA's dependency on particle size and measurement wavelength. x relates the mode diameter of the size distribution (d_{mode}) to the corresponding wavelength (λ) of optical measurements, i.e., λ = 375 nm for PAX, as shown in eq 2.

$$x_\lambda = \frac{\pi d_{mode}}{\lambda} \qquad (2)$$

2.3. Calculation of Refractive Index. RI values are measures of the interactions of a material with radiation. The RI consists of two components, a real component that describes scattering (n) and an imaginary component that describes absorption (k). RI values were calculated using an optical closure procedure and applying Mie theory (SI, section S3).[25−29] Variabilities reported in section 3.2 and Table 1, represent standard deviations of the measurements. Uncertainties were also estimated by forcing the RI calculation using instrumental uncertainties (SI, Table S2);[30] maximum uncertainties were $k^{+0.007}_{-0.005}$ and $n^{+0.08}_{-0.07}$ for pyrrole and $k^{+0.004}_{-0.002}$ and $n^{+0.09}_{-0.06}$ for thiophene. For furan experiments, n_{375} and k_{375} values were not calculated because the majority of $\beta_{abs,375}$ measurements were below or marginally higher than PAX detection limits.

2.4. Offline Optical Characterization. Aerosol samples were collected onto polytetrafluoroethylene membrane filters (Zefluor, Pall Laboratory, 47 mm, 1.0 μm pore size), after the particle volume concentration peaked. Filters were extracted in methanol and analyzed for UV−vis absorbance (Beckman DU-640). This process is further detailed in SI, section S4.

DOI: 10.1021/acs.estlett.9b00017
Environ. Sci. Technol. Lett. XXXX, XXX, XXX−XXX

2.5. Calculation of Mass Absorption Coefficient and Absorption Ångström Exponent. Calculation of the solution-based MAC from UV–vis spectra has been reported previously.[31,32] The effective MAC ($cm^2\ g^{-1}$) is calculated using eq 3.[31,32]

$$\mathrm{MAC}(\lambda) = \frac{\mathrm{A}(\lambda) \times \ln 10}{b \times C_{\mathrm{m}}} \quad (3)$$

where $\mathrm{A}(\lambda)$ is the absorbance at wavelength (λ) of filter extracts, b is the path length (1 cm), and C_m (g cm^{-3}) is the mass concentration of extracted SOA compounds in solution. C_m is determined by the filter sampling flow rate, average aerosol mass concentration during filter collection, sampling time, and extraction efficiency. The light-absorbing properties of aerosols are estimated by the average MAC ($\langle\mathrm{MAC}\rangle$) over the wavelengths range from λ_1 = 290 nm to λ_n = 700 nm).

$$\langle \mathrm{MAC} \rangle = \frac{\sum_{i=1}^{n} \mathrm{MAC}(\lambda_i)}{n} \quad (4)$$

To understand the wavelength dependence of light absorption, the absorption Ångström exponent (AAE) was calculated in the UV (290–400 nm) and visible (400–600 nm) ranges.[32]

$$\mathrm{AAE} = \frac{-\ln\left(\frac{\mathrm{MAC}(\lambda_1)}{\mathrm{MAC}(\lambda_2)}\right)}{\ln\left(\frac{\lambda_1}{\lambda_2}\right)} \quad (5)$$

2.6. Offline Chemical Characterization. The molecular composition of filter extracts was characterized using liquid chromatography (LC) coupled with a diode array detector (DAD) and a high-resolution time-of-flight mass spectrometer (HR-TOFMS, Agilent 6230 series). The instrument was equipped with an electrospray ionization source (ESI), and the detector was operated under the negative (−) ion mode. Further details can be found in SI, section S5.

3. RESULTS AND DISCUSSION

3.1. NO_3-Initiated SOA Formation from Heterocyclic Precursors. By assuming all of the injected VOC reacted with NO_3 radicals and propagating experimental uncertainties, the lower bound of SOA mass yields (SI, eq S3) were estimated to be 109 ± 29% for pyrrole, 7 ± 3% for furan, and 35 ± 8% for thiophene, assuming a density of 1.3 g cm^{-3}.[33] These values are estimates and are likely intercomparable, but caution should be used when comparing to more quantitative yield measures from other studies due to our small chamber size and potentially high particle wall-loss rates.

The low SOA mass production from furan is consistent with the low SOA yields from OH oxidation of furan reported in other studies.[34,35] Together these observations reveal that furan may not be a major contributor to SOA mass under a variety of common oxidation conditions. Conversely, the larger SOA mass formed from thiophene and pyrrole indicates that NO_3 chemistry with these compounds may be an important SOA source, particularly in biomass burning plumes where these compounds are readily found.[17]

3.2. Optical Properties of SOA. SSA_{375}, n_{375}, and k_{375} for pyrrole and thiophene experiments are displayed in Figure 1A,B. For the following discussion, SSA_{375} values are averaged for all measurements where $x_{375} > 1$ because the size dependency of SSA is expected to be minimal within this region.[36] The n_{375} values fell within the ranges previously observed for organic aerosols, with average values of 1.41 ± 0.05 and 1.44 ± 0.02 for pyrrole and thiophene SOA, respectively.

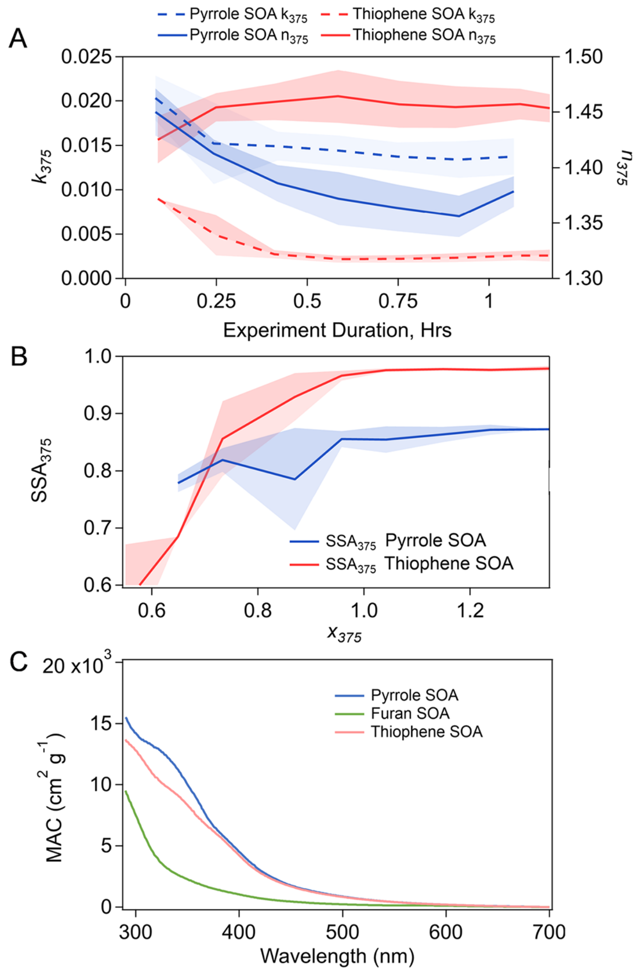

Figure 1. (A) Calculated refractive indices of pyrrole and thiophene SOA over the course of experiments. (B) Single scattering albedo values for pyrrole and thiophene relative to the size parameter at 375 nm (x_{375}). Values shown are averaged over all experiments for the given compound. Shaded areas represent 1 standard deviation and describe that variability between experiments. (C) Mass absorption coefficients (MAC) as a function of wavelength for pyrrole-, furan-, and thiophene-derived SOA.

Pyrrole SOA was the most absorbing among the three tested precursors, with an average SSA_{375} of 0.86 ± 0.01 and k_{375} of 0.015 ± 0.003. These values are similar to those previously observed for peat biomass burning (SSA_{375}, 0.93 and 0.85, and k_{375}, 0.009–0.015, depending on fuel packing density) by Sumlin et al.[37] Notably, the k_{375} values for pyrrole SOA decreased with exposure time and seem to be inversely related to SOA mass. This decrease in k_{375} could be driven by dilution of chromophores as more scattering components condense or by bleaching of existing chromophores. Bleaching might be driven by the oxidation of conjugated species by an oxidant (O_3 or NO_3) or particle phase processes such as hydrolysis of organonitrates.[38]

Thiophene SOA was slightly absorbing, with an average SSA_{375} of 0.98 ± 0.01 and k_{375} of 0.003 ± 0.002. Thiophene k_{375} values are similar to those observed by Liu et al.[21] for toluene SOA (k_{405} = 0.0041 ± 0.0005) and *m*-xylene SOA

DOI: 10.1021/acs.estlett.9b00017
Environ. Sci. Technol. Lett. XXXX, XXX, XXX–XXX

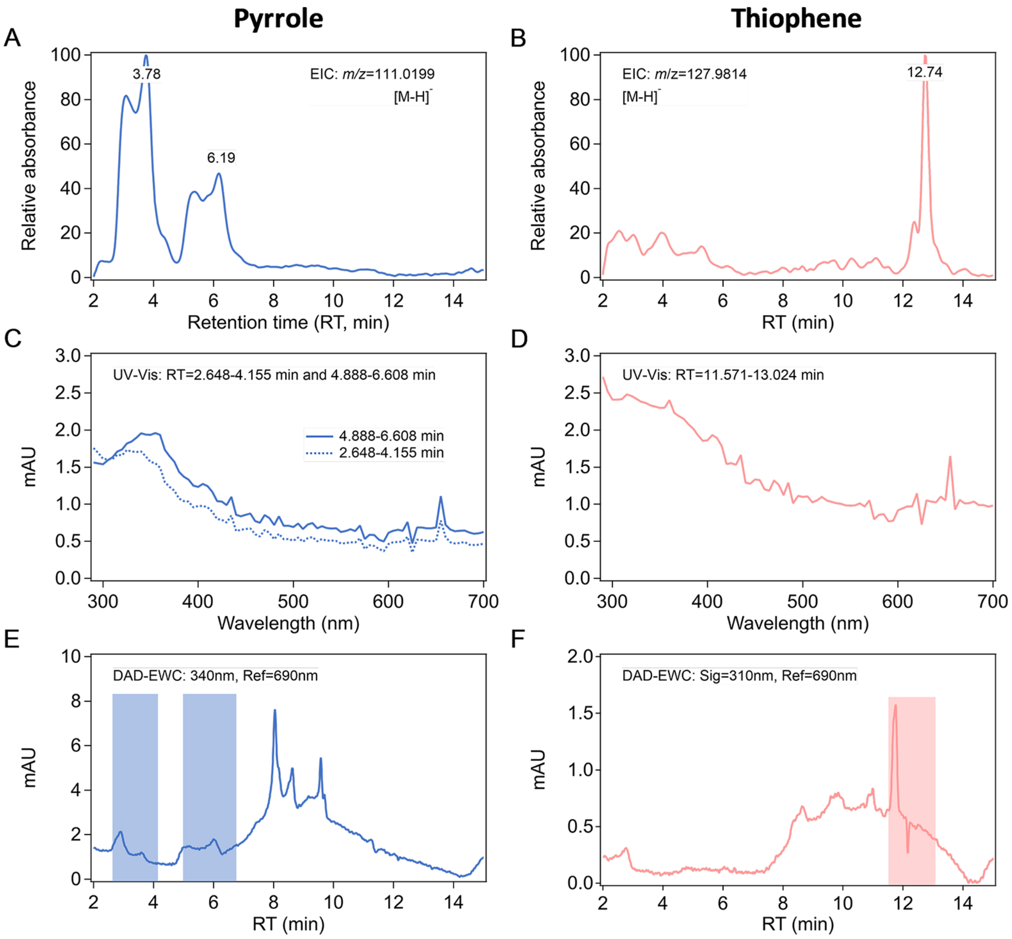

Figure 2. Extracted ion chromatograms (EICs) for (A) $C_4H_4N_2O_2$ in pyrrole SOA and (B) $C_4H_3NO_2S$ in thiophene SOA, the extracted UV−vis spectra (mAU, milli-Absorbance) of (C) pyrrole SOA at RT = 2.648−4.155 min and RT = 4.888−6.608 min and (D) thiophene SOA at RT = 11.571−13.024 min, and the extracted wavelength chromatograms (EWCs) for (E) pyrrole SOA and (F) thiophene SOA.

(k_{405} = 0.0030 ± 0.0003) formed from OH oxidation in the presence of NO_x.[21] These compounds are aromatic anthropogenic proxies, indicating that thiophene SOA products have similar absorption properties to SOA from anthropogenic precursors.

The majority of $\beta_{abs,375}$ measurements for furan SOA were below the PAX detection limit, which was likely caused by the low mass production of furan SOA in the chamber (section 3.1) and its low light absorption at 375 nm (section 3.3).

3.3. The Absorption Spectra of BrC. Similar to previously studied BrC SOA, samples collected from oxidation of unsaturated heterocyclic compounds absorb strongly in UV and near UV ranges, and the absorbance decreased as the wavelengths increased (Figure 1C).[15,16] The absorbance spectra of pyrrole and thiophene SOA showed a shoulder at ~330 nm. The $\langle MAC \rangle_{290-700}$ values of pyrrole, thiophene, and furan SOA were 3400 ± 700, 3000 ± 500, and 1100 ± 200 $cm^2\ g^{-1}$, respectively (Table 1). Notably, the offline MAC of furan SOA over the whole spectra and at 375 nm was significantly lower than in the other systems, which explains its negligible $\beta_{abs,375}$ values (section 3.2). These ⟨MAC⟩ are much higher than those of SOA (200−500 $cm^2\ g^{-1}$) derived from biogenic and anthropogenic VOCs under low or intermediate NO_x conditions but similar to the SOA from anthropogenic VOCs with high NO_x (VOC/NO_x < 5 ppbC/ppb) conditions (SI, Table S3).[31,39−41] No significant difference in AAE values was observed in the UV range. In the visible range, pyrrole (7.86 ± 0.45) and thiophene (7.60 ± 0.75) SOA showed higher AAE than that of furan SOA (5.42 ± 0.36), indicating their stronger wavelength dependence (Table 1).

3.4. Molecular Composition of BrC. Potential chromophores such as nitropyrrole ($C_4H_4N_2O_2$) and nitrothiophene ($C_4H_3NO_2S$) were observed in the SOA extracts by LC-DAD/ESI-HR-TOFMS (Figure 2A,B), and the presence of nitropyrrole in the gas phase was confirmed by the HR-ToF-CIMS data (SI, Figure S2). Nitrofuran was not detectable by LC/ESI-MS, likely due to the low mass yield of furan SOA. Isomers of nitropyrrole were present (i.e., 2- and 3-nitropyrrole), and the extracted ion chromatograms (EIC) showed two major peaks (3.78 and 6.19 min).

The extracted UV−vis spectra of pyrrole SOA (RT = 2.648−4.155 and 4.888−6.608 min) and thiophene SOA (RT = 11.571−13.024 min) showed significant absorption in the range of 300−350 nm (Figure 2C,D). For comparison, the UV−vis spectra of two standard compounds (i.e., 2-nitropyrrole and 2-nitrothiophene) were measured (SI, Figure S3) and peaked at 337 and 314 nm, respectively. These peaks are consistent with the substantial absorption by the corresponding extracts of pyrrole and thiophene SOA in similar wavelength ranges. Furthermore, the extracted wavelength chromatograms (EWC) of pyrrole and thiophene SOA (Figure 2E,F) peak at the times of nitropyrrole and nitrothiophene elution (Figure 2A,B). This evidence confirms the contribution

DOI: 10.1021/acs.estlett.9b00017
Environ. Sci. Technol. Lett. XXXX, XXX, XXX−XXX

of nitro-containing heterocyclic compounds and their isomers to the observed ⟨MAC⟩ values of SOA in this study.

Organonitrates are also potential chromophores in pyrrole and thiophene SOA. Liu et al. suggested that organonitrates could contribute significantly to the absorption of visible light.[7] In this study, organonitrates were not detected by LC/ESI-MS, probably due to the hydrolysis of ONO_2 groups in aqueous solutions during the sample workup and analysis procedure.[42] However, some organonitrates, such as nitrate-thiophene, nitrate-pyrrole, and nitrate-furan, were detected in the gas phase by HR-ToF-CIMS. (SI, Figure S2). Additionally, multiple unidentified absorption peaks in EWCs of pyrrole SOA (RT = 8−10 min) and thiophene SOA (RT = 9−11 min) reveal possible unknown chromophores.

3.5. Atmospheric Implications. This study demonstrates that the NO_3-initiated oxidation of unsaturated heterocyclic compounds is a source of secondary BrC. This pathway reveals a new source of nitroaromatic compounds in BrC aerosols and adds to our understanding of nighttime organic aerosol browning.[13,14] Considering the relatively high emission factors of pyrrole (up to 0.11 g/kg), thiophene (up to 0.01 g/kg), and furan (up to 0.31 g/kg) from burning of various fuels,[17] BrC from the oxidation of these precursors may be ubiquitous in biomass burning plumes.

To estimate the relative importance of each precursor to the ambient SOA and light absorption, the potential of SOA production (SOA_{pot}, g of SOA potentially produced per kg of fuel burned, SI, eq S4 and Table S4) and absorption cross-section emission factor (EF_{absC}, cm^2 of absorption per kg of fuel burned, SI, eq S5 and Table S5) were calculated for the six fuels burned by Hatch et al.,[17] assuming the precursors are all consumed through the NO_3 pathway. Pyrrole's SOA_{pot} is at least twice and its EF_{absC} is at least an order of magnitude more than those of furan and thiophene for tested fuels. The EF_{absC} of toluene, a VOC with a relatively high emission factor, was also estimated as a reference; pyrrole's SOA_{pot} and EF_{absC} are higher than those of toluene for these six fuels.[17,40,43] Furthermore, SOA_{pot} from the NO_3 oxidation of furan, pyrrole, and thiophene was 5−23% that of the SOA_{pot} from the OH oxidation of all biomass burning SOA precursors estimated by Hatch et al.[17] These results demonstrate that SOA from heterocyclic precursors, particularly pyrrole, may significantly contribute to nighttime SOA production and SOA light absorption.

Effects of nighttime atmospheric processing on heterocyclic VOCs and their potential to produce BrC SOA are currently understudied. Future research is warranted to quantify nitro and organonitrate products from this group of precursors in ambient samples, study their fates and reactivities, and model their formation processes.

■ ASSOCIATED CONTENT

Supporting Information

The Supporting Information is available free of charge on the ACS Publications website at DOI: 10.1021/acs.estlett.9b00017.

The calculation of refractive index, estimations of uncertainty in refractive index calculations, details of HR-ToF-CIMS measurements, the extraction of filters, the determinations of filter extraction efficiency, the procedures for LC-DAD-ESI-HR-TOFMS measurements, the calculations of SOA yields, the estimation of total potential SOA and absorption cross-section emission factors; estimated lifetimes of pyrrole, furan, and thiophene under our chamber conditions; uncertainties associated with the first and last *n* and *k* measurement; comparison of the ⟨MAC⟩ of SOA in this study with those of SOA in other studies; predicted contributions of pyrrole, furan, and thiophene released from biomass burning to the SOA production and light absorption; kinetic box model simulation of NO_3 radical production during the experiment; HR-ToF-CIMS time series of possible gas-phase nitro and nitrate compounds formed from the reaction between heterocyclic aromatic compounds and NO_3 radicals; MAC values of heterocyclic nitro compound standards including 2-nitropyrrole, 2-nitrofuran, and 2-nitrothiophene (PDF)

■ AUTHOR INFORMATION

Corresponding Author

*Phone: +1-951-827-3785. E-mail: ying-hsuan.lin@ucr.edu.

ORCID

Haofei Zhang: 0000-0002-7936-4493
Roya Bahreini: 0000-0001-8292-5338
Ying-Hsuan Lin: 0000-0001-8904-1287

Author Contributions

‖H.J. and A.L.F. contributed equally to this work

Notes

The authors declare no competing financial interest.

■ ACKNOWLEDGMENTS

This work was supported by the UCR Office of Research and Development Collaborative Seed Grant Program. We gratefully acknowledge use of the PAX instrument acquired with support from the National Science Foundation (AGS 1454374) and support from USDA (accession no. 1015963, project no. CA-R-ENS-5072-H). We thank Dr. Yongxuan Su for performing the LC-DAD-ESI-HR-TOFMS analysis using the Agilent 6230 accurate mass TOFMS instrument in the Molecular MS Facility at University of California San Diego (UCSD), which was funded by NIH Shared Instrument Grant (S10RR025636).

■ REFERENCES

(1) Pachauri, R. K.; Allen, M. R.; Barros, V. R.; Broome, J.; Cramer, W.; Christ, R.; Church, J. A.; Clarke, L.; Dahe, Q.; Dasgupta, P.; Dubash, N. K.; Edenhofer, O.; Elgizouli, I.; Field, C. B.; Forster, P.; Friedlingstein, P.; Fuglestvedt, J.; Gomez-Echeverri, L.; Hallegatte, S.; Hegerl, G.; Howden, M.; Jiang, K.; Jimenez Cisneroz, B.; Kattsov, V.; Lee, H.; Mach, K. J.; Marotzke, J.; Mastrandrea, M. D.; Meyer, L.; Minx, J.; Mulugetta, Y.; O'Brien, K.; Oppenheimer, M.; Pereira, J. J.; Pichs-Madruga, R.; Plattner, G. K.; Pörtner, H. O.; Power, S. B.; Preston, B.; Ravindranath, N. H.; Reisinger, A.; Riahi, K.; Rusticucci, M.; Scholes, R.; Seyboth, K.; Sokona, Y.; Stavins, R.; Stocker, T. F.; Tschakert, P.; van Vuuren, D.; van Ypserle, J. P. *Climate Change 2014: Synthesis Report; Contribution of Working Groups I, II and III to the Fifth Assessment Report of the Intergovernmental Panel on Climate Change*; IPCC, 2014.

(2) Feng, Y.; Ramanathan, V.; Kotamarthi, V. R. Brown Carbon: A Significant Atmospheric Absorber of Solar Radiation? *Atmos. Chem. Phys.* **2013**, *13* (17), 8607−8621.

(3) Lavi, A.; Lin, P.; Bhaduri, B.; Carmieli, R.; Laskin, A.; Rudich, Y. Characterization of Light-Absorbing Oligomers from Reactions of Phenolic Compounds and Fe(III). *ACS Earth and Space Chemistry* **2017**, *1* (10), 637−646.

(4) Zhang, X. L.; Lin, Y.-H.; Surratt, J. D.; Zotter, P.; Prevot, A. S. H.; Weber, R. J. Light-absorbing Soluble Organic Aerosol in Los Angeles and Atlanta: A Contrast in Secondary Organic Aerosol. *Geophys. Res. Lett.* **2011**, *38*, GL049385.

(5) Zhang, X. L.; Lin, Y.-H.; Surratt, J. D.; Weber, R. J. Sources, Composition and Absorption Ångström Exponent of Light-absorbing Organic Components in Aerosol Extracts from the Los Angeles Basin. *Environ. Sci. Technol.* **2013**, *47* (8), 3685−3693.

(6) Sun, H.; Biedermann, L.; Bond, T. C. Color of Brown Carbon: A Model for Ultraviolet and Visible Light Absorption by Organic Carbon Aerosol. *Geophys. Res. Lett.* **2007**, *34*, GL029797.

(7) Liu, S.; Shilling, J. E.; Song, C.; Hiranuma, N.; Zaveri, R. A.; Russell, L. M. Hydrolysis of Organonitrate Functional Groups in Aerosol Particles. *Aerosol Sci. Technol.* **2012**, *46* (12), 1359−1369.

(8) Nakayama, T.; Sato, K.; Matsumi, Y.; Imamura, T.; Yamazaki, A.; Uchiyama, A. Wavelength Dependence of Refractive Index of Secondary Organic Aerosols Generated during the Ozonolysis and Photooxidation of α-Pinene. *Sola* **2012**, *8*, 119−123.

(9) Lu, J. W.; Flores, J. M.; Lavi, A.; Abo-Riziq, A.; Rudich, Y. Changes in the Optical Properties of Benzo[a]pyrene-Coated Aerosols upon Heterogeneous Reactions with NO2 and NO3. *Phys. Chem. Chem. Phys.* **2011**, *13* (14), 6484−6492.

(10) Jacobson, M. Z. Isolating Nitrated and Aromatic Aerosols and Nitrated Aromatic Gases as Sources of Ultraviolet Light Absorption. *J. Geophys. Res-Atmos.* **1999**, *104* (D3), 3527−3542.

(11) Claeys, M.; Vermeylen, R.; Yasmeen, F.; Gómez-González, Y.; Chi, X.; Maenhaut, W.; Mészáros, T.; Salma, I. Chemical Characterisation of Humic-like Substances from Urban, Rural and Tropical Biomass Burning Environments using Liquid Chromatography with UV/vis Photodiode Array Detection and Electrospray Ionisation Mass Spectrometry. *Environ. Chem.* **2012**, *9* (3), 273−284.

(12) Desyaterik, Y.; Sun, Y.; Shen, X. H.; Lee, T. Y.; Wang, X. F.; Wang, T.; Collett, J. L. Speciation of "Brown" Carbon in Cloud Water Impacted by Agricultural Biomass Burning in Eastern China. *J. Geophys. Res.-Atmos.* **2013**, *118* (13), 7389−7399.

(13) Lin, P.; Bluvshtein, N.; Rudich, Y.; Nizkorodov, S. A.; Laskin, J.; Laskin, A. Molecular Chemistry of Atmospheric Brown Carbon Inferred from a Nationwide Biomass Burning Event. *Environ. Sci. Technol.* **2017**, *51* (20), 11561−11570.

(14) Bluvshtein, N.; Lin, P.; Flores, J. M.; Segev, L.; Mazar, Y.; Tas, E.; Snider, G.; Weagle, C.; Brown, S. S.; Laskin, A.; Rudich, Y. Broadband Optical Properties of Biomass-burning Aerosol and Identification of Brown Carbon Chromophores. *J. Geophys. Res-Atmos.* **2017**, *122* (10), 5441−5456.

(15) Laskin, A.; Laskin, J.; Nizkorodov, S. A. Chemistry of Atmospheric Brown Carbon. *Chem. Rev.* **2015**, *115* (10), 4335−4382.

(16) Moise, T.; Flores, J. M.; Rudich, Y. Optical Properties of Secondary Organic Aerosols and Their Changes by Chemical Processes. *Chem. Rev.* **2015**, *115* (10), 4400−4439.

(17) Hatch, L. E.; Luo, W.; Pankow, J. F.; Yokelson, R. J.; Stockwell, C. E.; Barsanti, K. C. Identification and Quantification of Gaseous Organic Compounds Emitted from Biomass Burning using Two-Dimensional Gas Chromatography-time-of-flight Mass Spectrometry. *Atmos. Chem. Phys.* **2015**, *15* (4), 1865−1899.

(18) Stockwell, C. E.; Yokelson, R.; Kreidenweis, S. M.; Robinson, A. L.; DeMott, P. J.; Sullivan, R. C.; Reardon, J.; Ryan, K. C.; Griffith, D. W.; Stevens, L. Trace Gas Emissions from Combustion of Peat, Crop Residue, Domestic Biofuels, Grasses, and Other Fuels: Configuration and Fourier Transform Infrared (FTIR) Component of the Fourth Fire Lab at Missoula Experiment (FLAME-4). *Atmos. Chem. Phys.* **2014**, *14* (18), 9727−9754.

(19) Brown, S. S.; Stutz, J. Nighttime Radical Observations and Chemistry. *Chem. Soc. Rev.* **2012**, *41* (19), 6405−6447.

(20) Atkinson, R.; Aschmann, S. M.; Winer, A. M.; Carter, W. P. Rate Constants for the Gas-phase Reactions of Nitrate Radicals with Furan, Thiophene, and Pyrrole at 295±1 K and Atmospheric Pressure. *Environ. Sci. Technol.* **1985**, *19* (1), 87−90.

(21) Liu, P.; Abdelmalki, N.; Hung, H. M.; Wang, Y.; Brune, W. H.; Martin, S. T. Ultraviolet and Visible Complex Refractive Indices of Secondary Organic Material Produced by Photooxidation of the Aromatic Compounds Toluene and m-Xylene. *Atmos. Chem. Phys.* **2015**, *15* (3), 1435−1446.

(22) Jenkin, M. E.; Saunders, S. M.; Wagner, V.; Pilling, M. J. Protocol for the Development of the Master Chemical Mechanism, MCM v3 (Part B): Tropospheric Degradation of Aromatic Volatile Organic Compounds. *Atmos. Chem. Phys.* **2003**, *3*, 181−193.

(23) Carter, W. P. L.; Crosley, D. R.; Golden, D. M.; Iraci, L. T.; Johnston, J. C.; Makar, P. A. *Atmospheric Chemistry and Chemical Mechanisms*; University of California, Riverside SRI International, Environment Canada, 1999; p 2.

(24) Carter, W. P. L. A Detailed Mechanism for the Gas-phase Atmospheric Reactions of Organic Compounds. *Atmos. Environ., Part A* **1990**, *24* (3), 481−518.

(25) Denjean, C.; Formenti, P.; Picquet-Varrault, B.; Katrib, Y.; Pangui, E.; Zapf, P.; Doussin, J. F. A new experimental approach to study the hygroscopic and optical properties of aerosols: application to ammonium sulfate particles. *Atmos. Meas. Tech.* **2014**, *7* (1), 183−197.

(26) Denjean, C.; Formenti, P.; Picquet-Varrault, B.; Camredon, M.; Pangui, E.; Zapf, P.; Katrib, Y.; Giorio, C.; Tapparo, A.; Temime-Roussel, B.; Monod, A.; Aumont, B.; Doussin, J. F. Aging of secondary organic aerosol generated from the ozonolysis of alpha-pinene: effects of ozone, light and temperature. *Atmos. Chem. Phys.* **2015**, *15* (2), 883−897.

(27) De Haan, D. O.; Hawkins, L. N.; Welsh, H. G.; Pednekar, R.; Casar, J. R.; Pennington, E. A.; de Loera, A.; Jimenez, N. G.; Symons, M. A.; Zauscher, M.; Pajunoja, A.; Caponi, L.; Cazaunau, M.; Formenti, P.; Gratien, A.; Pangui, E.; Doussin, J.-F. Brown Carbon Production in Ammonium- or Amine-Containing Aerosol Particles by Reactive Uptake of Methylglyoxal and Photolytic Cloud Cycling. *Environ. Sci. Technol.* **2017**, *51* (13), 7458−7466.

(28) Zarzana, K. J.; Cappa, C. D.; Tolbert, M. A. Sensitivity of Aerosol Refractive Index Retrievals Using Optical Spectroscopy. *Aerosol Sci. Technol.* **2014**, *48* (11), 1133−1144.

(29) Bohren, C. F.; Huffman, D. R. *Absorption and Scattering of Light by Small Particles*; John Wiley & Sons, 2008.

(30) Dingle, J. H.; Zimmerman, S.; Frie, A. L.; Min, J.; Jung, H.; Bahreini, R. Complex Refractive Index, Single Scattering Albedo, and Mass Absorption Coefficient of Secondary Organic Aerosols Generated from Oxidation of Biogenic and Anthropogenic Precursors. *Aerosol Sci. Technol.* **2019**, 1571680.

(31) Lin, Y.-H.; Budisulistiorini, S. H.; Chu, K.; Siejack, R. A.; Zhang, H.; Riva, M.; Zhang, Z.; Gold, A.; Kautzman, K. E.; Surratt, J. D. Light-Absorbing Oligomer Formation in Secondary Organic Aerosol from Reactive Uptake of Isoprene Epoxydiols. *Environ. Sci. Technol.* **2014**, *48* (20), 12012−12021.

(32) Chen, Y.; Bond, T. Light Absorption by Organic Carbon from Wood Combustion. *Atmos. Chem. Phys.* **2010**, *10* (4), 1773−1787.

(33) Nakao, S.; Tang, P.; Tang, X.; Clark, C. H.; Qi, L.; Seo, E.; Asa-Awuku, A.; Cocker, D. Density and Elemental Ratios of Secondary Organic Aerosol: Application of a Density Prediction Method. *Atmos. Environ.* **2013**, *68*, 273−277.

(34) Gomez Alvarez, E.; Borras, E.; Viidanoja, J.; Hjorth, J. Unsaturated Dicarbonyl Products from the OH-initiated Photo-oxidation of Furan, 2-Methylfuran and 3-Methylfuran. *Atmos. Environ.* **2009**, *43* (9), 1603−1612.

(35) Jiang, X.; Tsona, N. T.; Jia, L.; Liu, S.; Xu, Y.; Du, L. Secondary Organic Aerosol Formation from Photooxidation of Furan: Effects of NOx Level and Humidity. *Atmos. Chem. Phys. Discuss.* **2018**, *2018*, 1−27.

(36) Moosmuller, H.; Sorensen, C. M. Small and Large Particle Limits of Single Scattering Albedo for Homogeneous, Spherical Particles. *J. Quant. Spectrosc. Radiat. Transfer* **2018**, *204*, 250−255.

(37) Sumlin, B. J.; Heinson, Y. W.; Shetty, N.; Pandey, A.; Pattison, R. S.; Baker, S.; Hao, W. M.; Chakrabarty, R. K. UV-Vis-IR Spectral Complex Refractive Indices and Optical Properties of Brown Carbon Aerosol from Biomass Burning. *J. Quant. Spectrosc. Radiat. Transfer* **2018**, *206*, 392−398.

DOI: 10.1021/acs.estlett.9b00017
Environ. Sci. Technol. Lett. XXXX, XXX, XXX−XXX

(38) Hems, R. F.; Abbatt, J. P. D. Aqueous Phase Photo-oxidation of Brown Carbon Nitrophenols: Reaction Kinetics, Mechanism, and Evolution of Light Absorption. *Acs Earth and Space Chemistry* **2018**, *2* (3), 225−234.
(39) Updyke, K. M.; Nguyen, T. B.; Nizkorodov, S. A. Formation of Brown Carbon via Reactions of Ammonia with Secondary Organic Aerosols from Biogenic and Anthropogenic Precursors. *Atmos. Environ.* **2012**, *63*, 22−31.
(40) Liu, J.; Lin, P.; Laskin, A.; Laskin, J.; Kathmann, S. M.; Wise, M.; Caylor, R.; Imholt, F.; Selimovic, V.; Shilling, J. E. Optical Properties and Aging of Light-absorbing Secondary Organic Aerosol. *Atmos. Chem. Phys.* **2016**, *16* (19), 12815−12827.
(41) Nguyen, T. B.; Lee, P. B.; Updyke, K. M.; Bones, D. L.; Laskin, J.; Laskin, A.; Nizkorodov, S. A. Formation of Nitrogen- and Sulfur-containing Light-Absorbing Compounds Accelerated by Evaporation of Water from Secondary Organic Aerosols. *J. Geophys. Res-Atmos* **2012**, *117* (D1), JD016944.
(42) Baker, J. W.; Easty, D. M. Hydrolysis of Organic Nitrates. *Nature* **1950**, *166*, 156.
(43) Jiang, H.; Jang, M.; Yu, Z. Dithiothreitol activity by particulate oxidizers of SOA produced from photooxidation of hydrocarbons under varied NOx levels. *Atmos. Chem. Phys.* **2017**, *17* (16), 9965−9977.

DOI: 10.1021/acs.estlett.9b00017
Environ. Sci. Technol. Lett. XXXX, XXX, XXX−XXX